CONVOLUTIONAL SPATIAL FILTERING APPLIED TO PILOT POWER MEASUREMENTS

Fredrik Gunnarsson, IEEE Member

Department of Electrical Engineering
Linköpings universitet, SE-581 83 LINKÖPING, SWEDEN
Email: fred@isy.liu.se

ABSTRACT

Drive tests are important means to evaluate critical properties of a wireless network in operation. One is for example interested in coverage of the network, and therefore, the received power of a dedicated pilot signal is monitored to estimate the spatial variations of the power gain. With uniform time-sampling and a varying velocity, the typical temporal filter fails to extract the interesting information. In this paper we apply convolutional spatial filtering to resolve the problem, both causal and non-causal. Relations to spatial data analysis methods are also commented upon. Simulations indicate significant improvements.

1. INTRODUCTION

Spatial filtering and *spatial data analysis* are widely used within for example geographical information systems (GIS) and image processing [1]. Non-parametric applications include clustering of spatial data points or to addressing properties of spatial data aggregated to areal units such as countries. Another important field is to construct statistical models given irregularly sampled and noisy data points, perhaps to predict or interpolate values at other locations.

In general, spatial data is an example of *non-uniformly sampled signals*, typically in two or three dimensions. It can often also be seen as an *event-based sampled signal*, where the sample instants depend on when a triggering signal has reached a pre-defined threshold [2]. The triggering condition could be when the elapsed time since start has reached kT_s, i.e. a uniformly time-sampled signal. When measuring a spatial quantity while traveling with a time-varying velocity, the spatial data will be non-uniformly sampled in space (and also event-based sampled).

One example of such a signal is pilot power measurements from drive tests in terrestrial wireless networks. Each base station in such a network typically transmits a pilot signal to support channel estimation in mobiles and to support the determination of the most favorable base station to connect to at the location of the mobile. When deploying and tuning networks, cell planning software predicting radio propagation helps out, but comprehensive drive tests are also needed to verify the coverage of the network. Since it is impossible to maintain a constant velocity, the measured pilot power is an example of a uniformly time-sampled and non-uniformly space-sampled spatial signal. With dedicated test equipment, the received pilot power is made readily available together with geographical positions using GPS. Ordinary mobiles report quantities related to the pilot signal quality, and statistical methods to extract relevant information from readily available mobile measurements are discussed in [3].

In this paper, practical spatial filtering is intuitively motivated as discretizing a space-continuous linear filter, either causal or non-causal. It is related to the weighted averaging and the kernel estimation techniques used for smooting and interpolation in spatial data analysis [1]. With the linear filtering approach, it is natural to associate the spatial filtering to the spatial frequency properties of the studied signal. Thus, the choice of filter depend on the signal characteristics. The filtering methods in spatial data analysis also relate to the theory of splines used for data interpolation [4]. Other popular approaches include wavelet transform methods, see for example [5].

Section 2 models the pilot power signal and addresses its typical characteristics. Spatial filtering is described in Section 3 together with some implementational aspects. The filter performance is illustrated by simulations in Section 4, and Section 5 summarizes with conclusive remarks.

2. SIGNAL MODEL

The general notation of a uniformly time-sampled and non-uniformly space-sampled signal is described in Section 2.1. Many test mobiles are based on ordinary mobiles, but with interfaces to report measurements more frequent. Typically, the measurements reflect the time-varying channel and/or the interferencing signals. This is discussed in more detail in Section 2.2. The last subsection addresses characteristics of signals from drive tests.

2.1. Notation

In general we have a time sampled signal $u[t]$ with sample instants $t = 1,\ldots,N$ and sample interval T_s. Furthermore, GPS information is used to compute the relative distance between samples, and that the signal is spatially related $u(d_t)$ to the travelled distance d_t at time instant t. With a time-varying velocity $v(t)$, the travelled distance is thus

$$d_t = d_{t-1} + \int_{t-1}^{t} |v(\tau)| d\tau$$

The spatially filtered measurements are denoted $y(d_t)$.

This work is supported by the competence center ISIS, Linköpings universitet, and in cooperation with Ericsson Research, which all are acknowledged.

2.2. Mobile Station Measurements

The measurement capabilities of an UMTS mobile is specified in [6]. There are primarily two defined measurement quantities that relate to the pilot signal - the received pilot power and the pilot power relative to the power of all other signals and noise.

The base station transmits the pilot signal with the power P_{pilot} (about 1 W). By averaging fast varying effects on data symbol and chip level, the communication channel between the base station and the mobile can be seen as a space varying power gain, $g(d)$. Moreover, the mobile also receives interfering signals with power I_0. The mobile is capable of measuring both

$$P_{\text{pilot}}g(d) \quad \text{and} \quad \frac{P_{\text{pilot}}g(d)}{I_0}$$

The power gain is often separated into three components $g(d) = g_p(d)g_s(d)g_m(d)$, or in decibels $g^{\text{dB}}(d) = g_p^{\text{dB}}(d) + g_s^{\text{dB}}(d) + g_m^{\text{dB}}(d)$, see Figure 1

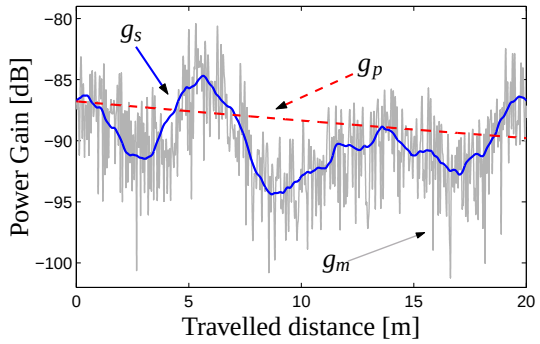

Fig. 1. The power gain $g(t)$ is modeled as the sum of three components: path loss $g_p(t)$, shadow fading $g_s(t)$ and multipath fading $g_m(t)$. Here this is illustrated when moving from a reference point and away from the transmitter.

The received signal power decreases with the distance to the base station, and the path loss is modeled as $g_p = K - \alpha \log_{10}(d)$ when traveling directly away from the base station. Terrain variations cause diffraction phenomenons and this shadow fading g_s is modeled as $ARMA(n,m)$-filtered Gaussian white noise (n is typically 1-2, $m = n-1$, [7]). Path loss and shadow fading have been subject to extensive empirical analysis, see for example [8, 9, 10]. In terms of spatial frequency, the shadow fading has its frequency content below 0.01 - 1 m^{-1} [11] depending on the terrain.

The multipath model considers scattering of radio waves, yielding a rapidly varying gain g_m [12, 13]. In suburban and urban areas, the *line-of-sight (LoS)* path is sometimes blocked by buildings. The received signal has therefore no dominating component. Instead it receives many incident components due to near-field scattering, where the signals are reflected by a large number of objects close to the receiver. This causes fast variations of the signal amplitude known as *fast fading*. There are a number of reference fast fading channel models defined by UMTS the standardization body [14].

The measurements will be represented in decibels, and the fast fading is thus considered as an additive disturbance. Since the main focus is to filter out fast fading without affecting the shadow fading variations, the path loss component is mainly constant on the considered time scale and is left out. Since the transmitted pilot power and the interference also can be considered constant, the focus is on spatially filtering the power gain.

2.3. Measured Pilot Power Characteristics

The measurements discussed hitherto are important when assigning the most appropriate base station for ordinary mobiles. To avoid ping-pong effects, where mobiles are re-assigned frequently to different base stations, the measurements are filtered to only reflect the path loss and the shadow fading. It is therefore also interesting for drive tests to record the most favorable base station on average. The measurements are also used to improve the propagation models in planning tools, which typically models path loss and shadow fading, and only considers the effects of fast fading by margins. To average out fast fading, measurements are filtered using a temporal filter. This works fine when the velocity is rather constant, but fails when the velocity varies. For example see Figure 2a, where the vehicle stop e.g., at a set of traffic lights in the middle of the drive test. As seen in Figure 2b, the temporal filter manage to filter out the fast fading when traveling at moderate speeds, but fails at low speeds, and the fast fading contribution is evident.

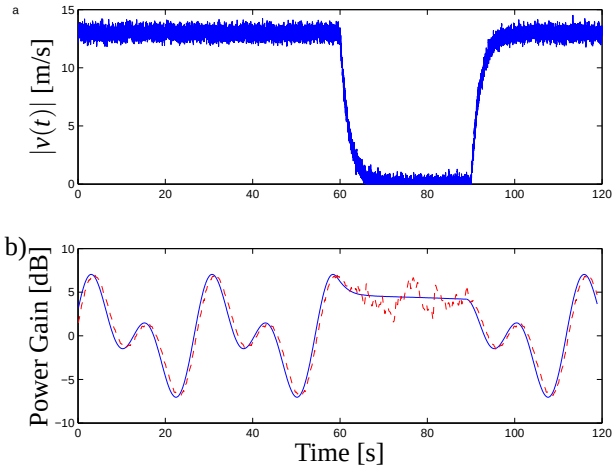

Fig. 2. Signals used in the simulations. a) Time-varying velocity emulating a stop at a set of traffic lights, b) Resulting measurements (dashed) and the true shadow fading envelope (solid).

Together with mobile station measurements, a GPS receiver keeps track of the spatial location. The absolute location measurements are rather crude, but the relative distance between measurements can be computed more accurately.

3. SPATIAL FILTERING

Many techniques for spatial filtering tailored for different applications and more general exist. We bring up two general techniques from literature, and relate them to the proposed convolutional spatial filtering. Ordinary averaging fails as indicated by Figure 2b, but *weighted averaging* [1] considering

the relative distance between samples is more applicable

$$y(d_t) = \sum_{\tau=1}^{N} w(|d_t - d_\tau|)u(d_t) \quad (1)$$

with $\sum_{\tau=1}^{N} w(|d_t - d_\tau|) = 1$. The weights typically are chosen as

$$w(x) \propto x^{-\alpha} \quad \text{or} \quad w(x) \propto e^{-\alpha x} \quad (2)$$

where α is related to the amount of smooting. Often, $w(x) = 0, x \geq d_{\max}$.

In *kernel estimation* [1], the smoothed estimate is computed as

$$y(d_t) = \frac{\sum_{\tau=1}^{N} \kappa\left(\frac{d_t - d_\tau}{\beta}\right) u(d_\tau)}{\sum_{\tau=1}^{N} \kappa\left(\frac{d_t - d_\tau}{\beta}\right)} \quad (3)$$

where $\kappa(\cdot)$ is the *kernel*. The parameter β determines the amount of smooting (essentially the interval around d_t within which data points significantly will contribute to the estimate). A popular choice is a quadratic kernel

$$\kappa(x) = \begin{cases} \frac{3}{\pi}(1-x^2) & x^2 < 1 \\ 0 & \text{otherwise} \end{cases} \quad (4)$$

If we assume that the measured signal $u(d)$ is continuous in space, it is natural to employ a linear filter with impulse response $h(d)$. The estimate is given by the convolution

$$y(d) = \int_{-\infty}^{d} h(\delta - d)u(\delta)d\delta \quad (5)$$

The estimate at d_t can be approximated by representing the integral by its Riemann sum

$$y(d_t) \approx \sum_{\tau=-\infty}^{t} (d_\tau - d_{\tau-1})h(d_\tau - d_t)u(d_\tau) \quad (6)$$

With normalization:

$$y(d_t) = \frac{\sum_{\tau=-\infty}^{t}(d_\tau - d_{\tau-1})h(d_\tau - d_t)u(d_\tau)}{\sum_{\tau=-\infty}^{t}(d_\tau - d_{\tau-1})h(d_\tau - d_t)} \quad (7)$$

A simple filter example is the following first order filter

$$H(s) = \frac{1}{sD+1}, \quad h(d) = e^{-d/D} \quad (8)$$

with the parameter D. The is intuitively appealing, since the parameter D is equal to the decorrelation distance (correlation equal to $e\ -1$) and the filter bandwidth is $1/D$ m -1. Figure 3 illustrates convolutional spatial filtering using the filter in (8). With the convolutional approach, it is natural to relate the filtering properties such as the bandwidth to the spatial frequency content of the interesting signal. The filter length can be made finite by specifying a maximum distance $d_{\max}$ of the filter or a minimally considered correlation c. Note that these quantities are related by (8):

$$c = e^{-d_{\max}/D}$$

The filter in (7) is causal and applicable to real-time processing. A typical case is that the data can be post-processed after the drive test. To obtain a non-causal and zero-phase version of the we use the fact that if $H^{\mathrm{c}}(z)$ is a causal filter, then the non-causal filter

$$H^{\mathrm{nc}}(z) = H^{\mathrm{c}}(z)H^{\mathrm{c}}(z^{-1})$$

is zero-phase. Using the alternative representation of the spatial signals $u[t]$ and $y[t]$ (which is more implementationally appealing) this can be implemented as follows.

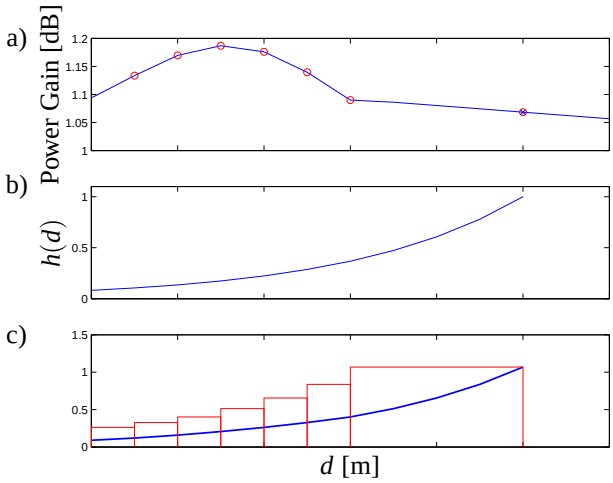

Fig. 3. Convolutional spatial filtering. a) Space continuous shadow fading component (solid), measurements (circles) and one measurement to be filtered (star), b) Filter impulse response, c) Riemann approximation of the integral in (6).

Algorithm 1 (Non-causal Spatial Filtering)

1. $y^c[t] = \frac{\sum_{\tau=-\infty}^{t}(d_\tau - d_{\tau-1})h(d_\tau - d_t)u[\tau]}{\sum_{\tau=-\infty}^{t}(d_\tau - d_{\tau-1})h(d_\tau - d_t)}$
2. Reverse signals $d_t^{nc} = d_N - d_{N+1-t}$ and $u^{nc}[t] = y^c[N+1-t]$.
3. $y^{nc}[t] = \frac{\sum_{\tau=-\infty}^{t}(d_\tau^{nc} - d_{\tau-1}^{nc})h(d_\tau^{nc} - d_t^{nc})u^{nc}[\tau]}{\sum_{\tau=-\infty}^{t}(d_\tau^{nc} - d_{\tau-1}^{nc})h(d_\tau^{nc} - d_t^{nc})}$
4. Re-reverse the result $y[t] = y^{nc}[N+1-t]$

Clearly, the weighted averaging (1) and kernel estimation (3) and the non-causal convolutional algorithm above are essentially identical. The main reasons for using the linear filtering framework is educational and that it is more natural to relate the filter to signal properties.

4. SIMULATIONS

Consider the situation in Figure 2, where the measured signal is strongly affected by the temporary stop at the traffic lights. (The velocity i s first roughly constant, then exponentially decreased to roughly zero for a while, and finally exponentially increasing to the initial level.). The simulated shadow fading components have frequency components up to 0.07 m^{-1} (essentially two sinusoids). Power gain is measured at 1500 Hz (once per slot in UMTS), low-pass filtered and the measurements are decimated to the sample interval T_s=0.1 s. Fast fading is modeled using the Typical Urban channel model [14].

The first order filter in (8) is used for convolutional spatial filtering of the measurements.

Figure 4 illustrate the performance over time and in comparison to the true shadow fading envelope. The temporal low-pass filter in the test mobile causes a group delay as seen in Figure 4a. This delay is increase with causal filtering in Figure 4b, but the fast fading components are essentially filtered out. The short extra delay have little spatial effect and no effect on the statistical shadow fading analysis. This additional delay is however remove when employing the non-causal zero-phase filter in Algorithm 1.

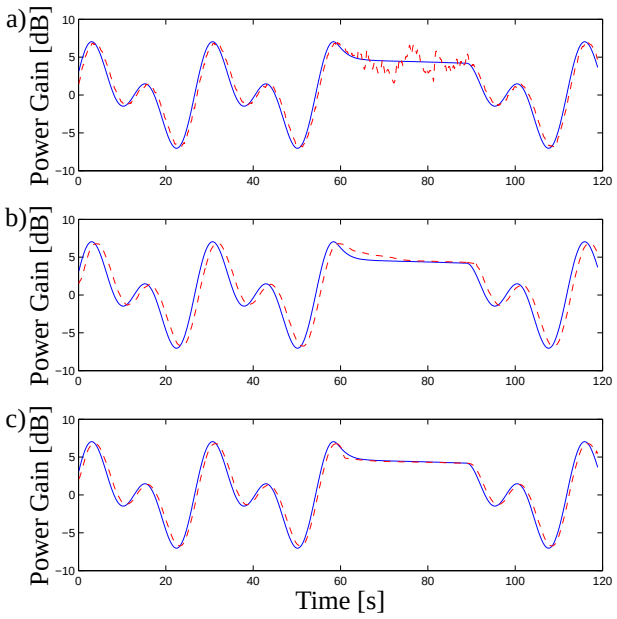

Fig. 4. True shadow fading (solid) and measurement/estimate (dashed) a) Measured signal, b) Causally filtered measurement, c) Non-causally filtered measurement.

The estimated shadow fading envelope is close to the true envelope as seen in Figure 5, where the envelopes ate depicted relative travelled distance.

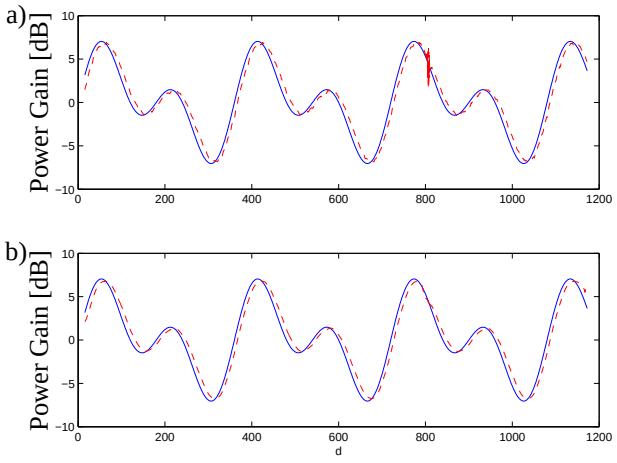

Fig. 5. True shadow fading (solid) and measurement/estimate (dashed) with respect to distance a) Measured signal, b) Non-causally filtered measurement.

5. CONCLUSIONS

With uniformly time-sampled, but non-uniformly space sampled signals, it is difficult to suppress noise with temporal filters. In this work, the applicability of convolutional spatial filters is explored and simulation results are promising. The simulations indicate that spatial post-processing can recover the interesting signals with a causal filter, and even better with a zero-phase non-causal filter. The filter approach allow intuitive interpretations of parameters, and it is natural to relate to channel characteristics of the wireless link. Relations to spatial data analysis methods are also commented upon.

6. REFERENCES

[1] A. S. Fotheringham, C. Brunsdon, and M. Charlton. *Quantitative Geography – Perspectives on Spatial Data Analysis*. Sage, London, UK, 2000.

[2] K. J. Astrom and B. Bernhardsson. Comparison of periodic and event based sampling for fi rst-order stochastic systems. In *Proc. IFAC World Congress*, Beijing, P. R. China, July 1999.

[3] J. Blom, F. Gunnarsson, and F. Gustafsson. Estimation in cellular radio systems. In *Proc. IEEE International Conference on Acoustics, Speech, and Signal Processing.*, Phoenix, AZ, USA., March 1999.

[4] M. Unser. Splines - a perfect fi t for signal and image processing. *IEEE Signal Procesing Magazine*, 16(6), Nov 1999.

[5] R. Öktem and K. Egiazarian. A wavelet transform method for coding fi lm-grain noise corrupted images. In *Proc. IEEE International Conference on Acoustics, Speech, and Signal Processing.*, Istanbul, Turkey, May 2000.

[6] 3GPP Technical Specifi cation Group Radio Access Network. Requirements for support of radio resource management. Technical report 3G TS 25.133, 2000.

[7] T.B. Sørensen. Correlation model for slow fading in a small urban macro cell. In *Proc. IEEE Personal, Indoor and Mobile Radio Communications*, Boston, MA, USA, September 1998.

[8] M. Gudmundson. Correlation model for shadow fading in mobile radio systems. *IEE Electronics Letters*, 27(23), 1991.

[9] M. Hata. Empirical formula for propagation loss in land mobile radio services. *IEEE Transactions on Vehicular Technology*, 29(3), 1980.

[10] Y. Okamura, E. Ohmori, T. Kawano, and K. Fukuda. Field strength and its variability in VHF and UHF land-mobile radio service. *Review of the Electrical Communication Laboratory*, 16(9-10), 1968.

[11] F. Gunnarsson. *Power Control in Cellular Radio System: Analysis, Design and Estimation*. PhD thesis, Linköpings universitet, Linköping, Sweden, April 2000.

[12] B. Sklar. Rayleigh fading channels in mobile digital communication systems. *IEEE Communications Magazine*, 35(7), 1997.

[13] R.H. Clarke. A statistical theory of mobile-radio reception. *The Bell System Technical Journal*, 47(6), July-August 1968.

[14] 3GPP Technical Specifi cation Group Radio Access Network. Deployment aspects. Technical report 3G TS 25.943, 2000.